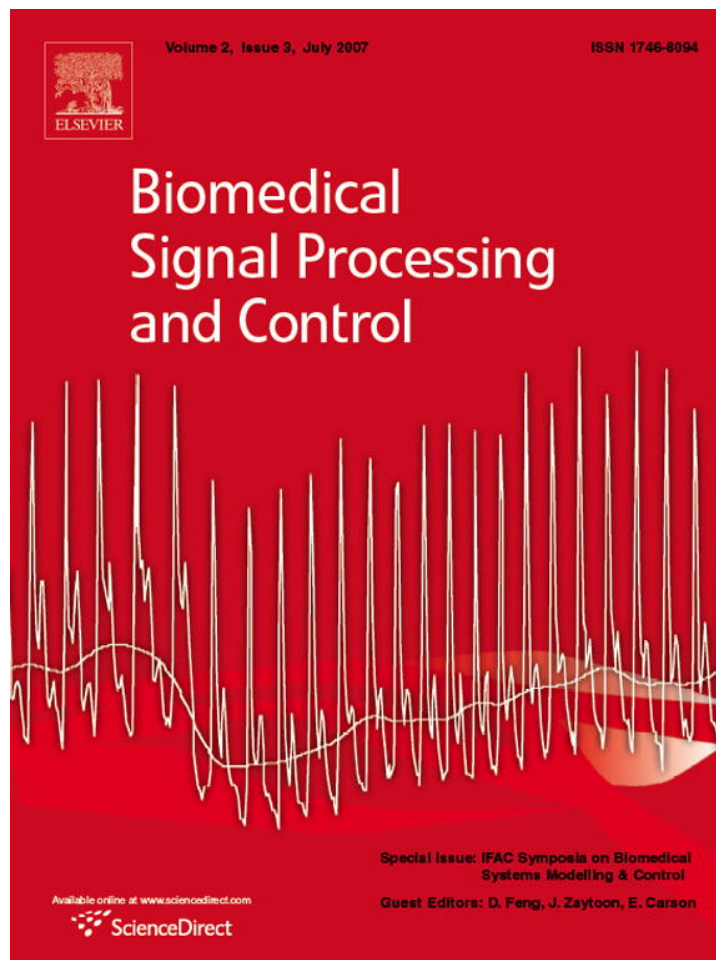


Provided for non-commercial research and education use.
Not for reproduction, distribution or commercial use.



This article was published in an Elsevier journal. The attached copy is furnished to the author for non-commercial research and education use, including for instruction at the author's institution, sharing with colleagues and providing to institution administration.

Other uses, including reproduction and distribution, or selling or licensing copies, or posting to personal, institutional or third party websites are prohibited.

In most cases authors are permitted to post their version of the article (e.g. in Word or Tex form) to their personal website or institutional repository. Authors requiring further information regarding Elsevier's archiving and manuscript policies are encouraged to visit:

<http://www.elsevier.com/copyright>



ELSEVIER

Available online at www.sciencedirect.com

Biomedical Signal Processing and Control 2 (2007) 180–190

Biomedical
Signal Processing
and Control

www.elsevier.com/locate/bspc

Isometric muscle contraction induced by repetitive peripheral magnetic stimulation (RPMS)—Modeling and identification

Michael Bernhardt^{a,b,*}, Bernhard Angerer^b, Martin Buss^a, Albrecht Struppler^b

^a*Institute of Automatic Control Engineering, Technische Universität München, Theresienstr. 90, 80290 München, Germany¹*

^b*Research Group for Sensorimotor Integration, Klinikum Rechts der Isar of the Technische Universität München, Germany²*

Received 27 February 2007; received in revised form 22 May 2007; accepted 9 July 2007

Available online 30 August 2007

Abstract

Repetitive peripheral magnetic stimulation (RPMS) is an innovative approach in treatment of central paresis, e.g. after stroke. In this article we present a neuromuscular model for the RPMS-induced isometric muscle contraction. This model is the basis for our two recent goals in research: improvement and assessment of the RPMS therapy by means of position controlled induction of functional movements and with automated system identification based therapy evaluation. In order to adapt the model parameters to the individual a nonlinear on-line system identification method is proposed. Physiological systems may be complex and detailed so that in many cases macroscopic models of the dominant characteristics are built. Therefore, mathematical descriptions of these models and respective parameter identification methods have to cope with uncertainties. This paper presents a separable nonlinear regression model of Hammerstein structures that maximizes the possibility of incorporation of a priori knowledge and is still flexible to structural uncertainties. A robust on-line identification method based on the Levenberg–Marquardt algorithm is presented that works in a reduced parameter space, due to the separability of the model equation.

© 2007 Elsevier Ltd. All rights reserved.

Keywords: Stroke rehabilitation; Neuromuscular model; System identification; Separable least squares

1. Introduction

A central paresis of the arm and/or hand, e.g. after stroke, reduces the quality of life dramatically. Studies on large clinical cohorts, using standard therapeutic methods, showed that approximately 90% of stroke patients have persistent hemiparesis of the upper extremities, and in 30–40% the paresis is so severe that the affected limb can not be used any more. This data emphasizes the necessity of innovative approaches in rehabilitation of central paresis.

Cortical reorganization abilities form the basis of relearning lost motor functions. In order to activate a beneficial reorganization process, the lost proprioceptive input should be reactivated. Currently, physiotherapy aims to achieve such an activation through externally applied movements. Inducing the lost movement via muscle stimulation results in a higher

proprioceptive input which corresponds closer to the lost voluntary action patterns. Ultimately, this leads to an increase in the therapeutic effect [1].

In this context functional electrical stimulation (fES) is a well-known method. Though the fES activates somatosensory nerve fibers a major drawback consists of the equal activation of the cutaneous receptors. Apart from leading to pain this may also result in an additional increase in spasticity. Hence, the use of fES for therapeutic purposes appears limited, see e.g. [2].

In order to achieve a deeper penetrating, focused and painless stimulation we use the new method of repetitive peripheral magnetic stimulation (RPMS) (see Fig. 1). The repetitively applied field impulses are sinusoidal half-waves with a fixed duration of 100 μ s and a variable amplitude called stimulation intensity.

The therapeutic concept of RPMS is the activation of a reorganization process by inducing a proprioceptive input to the central nervous system (CNS), physiologically corresponding to the lost input during active movements, e.g. [1]. In clinical experimental studies [3] on spasticity, cognitive functions, cerebral activation, stiffness around the elbow joint and goal-

* Corresponding author. Tel.: +49 89 289 23415; fax: +49 89 289 28340.

E-mail address: bernhardt@tum.de (M. Bernhardt).

¹ <http://www.lsr.ei.tum.de>.

² <http://www.netstim.de>.

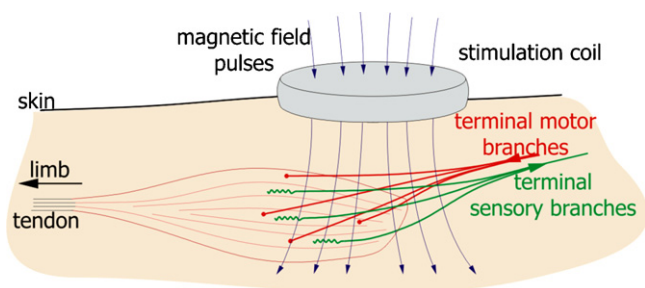


Fig. 1. Principle of the RPMS application.

directed motor performances, it was shown, that the sensorimotor dysfunctions due to brain lesions can improve remarkably with the application of RPMS.

Our current research focuses on the improvement and the assessment of RPMS-therapy.

Fig. 2 summarizes our main aims:

- Optimization of the proprioceptive inflow by inducing position controlled functional movements with multiple coils.
- Time continuous tracking of patient parameters like level of spasticity and muscle fatigue based on system identification.

As a basis for these research goals a neuromuscular model of the RPMS-induced muscle contraction has to be developed. Modeling and identification of the muscle contraction behavior has already been investigated for fES (see e.g. [4–6]). Since there are fundamental differences in pulse shape as well as in pulse propagation of fES and RPMS, the induced muscle responses might also differ from one another.

For extraction of patient parameters during therapy, the system has to be identified under non-isometric conditions. For this purpose the system input u (magnetic field pulses) and the system output y (joint angle of the respective limb) have to be measured and used to adapt the parameters of an underlying model by minimizing the output error. Time varying components of this plant are muscle fatigue and spasticity. In [7] a pilot study on spasticity quantification during RPMS is described. In this article, an identification under isometric condition is considered where the length of the stimulated

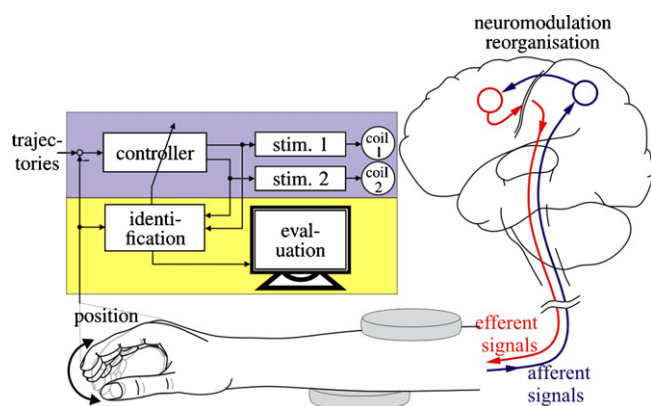


Fig. 2. Overview of the main research goals.

muscle is nearly unchanged and the muscle force is the measured system output. Under isometric conditions the force generation of a stimulated muscle can be investigated separately. This is an important basis for further research. Having the above mentioned applications in mind, the identification of isometric muscle contractions has been implemented as on-line algorithm, too.

Models of physiological systems often have a macroscopic character since the underlying microscopic (e.g. biochemical) processes may be too complex for a detailed model. Therefore, parts of the models may be inconsistent with the real plant which leads to structural uncertainties. The mathematical formulation of model equation has to address these uncertainties by making use of a priori knowledge as far as it exists, and be flexible with respect to system structure and parameters where a priori knowledge is poor.

Further challenges in identification of physiological systems are time variance and inter- and intrapersonal differences. Hence, model parameters have to be adapted to the respective subject, once a qualitative model is found.

In this paper, first a Hammerstein model (see Fig. 3) of the RPMS-induced isometric muscle contraction is developed based on experimental data taken from the musculus biceps brachii. The obtained model yields qualitative knowledge about the basic shape of $n(u)$ and about order and time constants of the LTI-system.

In order to adapt the model parameters to the respective subject, a gray box identification approach has been developed that is based on the separable nonlinear least-squares methods [8,9]. The developed model equation approximates the static nonlinearity of the Hammerstein structure by a parameterized nonlinear function of similar shape. The LTI-system is approximated by a truncated convolution sum. Hence, the incorporation of a priori knowledge for the identification process is maximized, without predefining the model order. For robust on-line identification a modified recursive Levenberg–Marquardt algorithm [10] is presented.

2. Isometric contraction model

The force generated by a muscle that is stimulated with magnetic pulses under isometric conditions will be modeled. According to the approaches used with fES [4] the dynamic behavior (activation dynamics) as well as static behavior (recruitment characteristics) will be analyzed. In order to obtain experimental data, a setup as depicted in Fig. 4 has been used. A stimulation coil (a surface electrode for fES, respectively) is placed above the innervation area of the musculus biceps brachii, and the force resulting from stimulation is measured with a force sensor attached to the subject's wrist. In order to

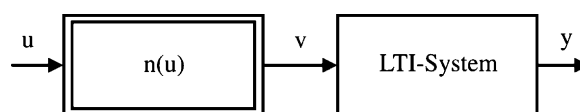


Fig. 3. Hammerstein cascade: a block structured nonlinear system that consists of a static nonlinearity in series with an LTI system.

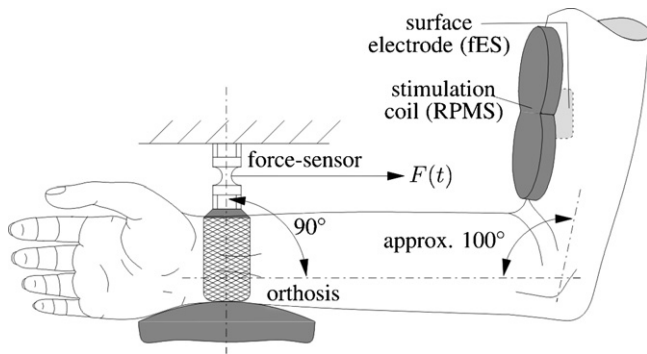


Fig. 4. Measuring the force response under isometric conditions during RPMS and during fES, respectively. A small focusing fES-electrode has been placed above the m. biceps brachii. The indifferent electrode has been placed at the dorsal side of the upper arm.

compare RPMS with fES, all experiments concerning the activation dynamics have been accomplished with electrical stimulation as well. For RPMS, the maximum stimulation intensity of 100% corresponds to a magnetic flux density of approximately 2.0 T. For fES, maximum stimulation intensity was achieved with a pulse width of 200 μ s and a stimulation current at the maximum tolerable threshold of pain of the respective subject.

2.1. Activation dynamics

The activation dynamics denote the dynamic force response $F(t)$ of the respective muscle due to stimulation $u(t)$. First, we investigate the dynamics of a muscle twitch caused by a single stimulus and derive an appropriate LTI-model $G_a(s) = F(s)/u(s)$. Important parameters are the time delay T_1 between the peripheral stimulus and the mechanical muscle response as well as the structure, order and time constants T_a of $G_a(s)$.

In order to determine the time delay T_1 force responses to single magnetic pulses have been analyzed. The raw force signal $F_{\text{raw}}(t)$ shows an artifact due to the strong magnetic pulse. The maximum of this artifact is taken to determine the particular time of the peripheral stimulus. The start of the muscle twitch is defined as last positive zero crossing of $\dot{F}(t)$. The time derivative $\dot{F}(t)$ is obtained by numerical differentiation of the filtered signal $F_{\text{filtered}}(t)$. In order to avoid phase shift, forward-backward filtering has been applied with the moving average filter $F_{\text{filtered}}(t) = \sum_{k=0}^N F_{\text{raw}}(t - kT_s)$, $N = 8$, $T_s = 1$ ms. In order to determine the average time delay \bar{T}_1 , 3698 data sets of 8 healthy subjects (aged from 20 to 32 years) with different stimulation intensities and pulse widths have been evaluated.

The results are summarized in Table 1. A significant dependency of T_1 on the stimulation intensity and stimulation pulse width, respectively, could not be shown.

As a model of the force response, in fES related work typically a second-order transfer function with two identical real poles at $-1/T_a$ is proposed. In the following, a transfer function of n th order with identical real poles is considered. The poles have to be real, since no oscillations in the force

Table 1

Time delay T_1 , mean value \bar{T}_1 and mean standard deviation \bar{s}_{T_1} over all subjects

	Electr. stim.	Magnetic stim.
T_1 (ms)	20.83–28.24	6.28–14.63
Mean value \bar{T}_1 (ms)	24.4	9.45
\bar{s}_{T_1} (ms)	3.05	1.12

responses have been observed. Hence, we obtain a transfer function $G'_a(s)$ and as time domain equation of its step response.

When normalizing the time domain Eq. (1) so that the maximum value is 1 the modeled force response can be written as

$$\hat{F}(T_a, t) = \frac{(t)^{n-1} e^{-t/T_a}}{((n-1)T_a)^{n-1} (n-1) e^{-(n-1)}}. \quad (2)$$

Thus, the normalized function $\hat{F}(T_a, t)$ can be compared with the normalized force response $F(t)/F_{\text{max}}$, whereas F_{max} is the maximum value of the respective measured muscle twitch. In order to evaluate the approximation of Eq. (2), the quadratic error

$$E(T_a) = \sum_{k=0}^N \left(\frac{F[k]}{F_{\text{max}}} - \hat{F}(T_a)[k] \right)^2 \quad (3)$$

is defined, whereas N is the length of the truncated force response and $k = t \cdot f_s$ is the discretized time after sampling with the sample rate f_s . The optimal time constant $T_{a,\text{opt}}$ is computed by minimizing $E(T_a)$ with a recursive search algorithm. 3143 data sets with different stimulation intensities and pulse widths have been evaluated. First, it could be shown that neither with fES nor with RPMS the pulse width of the applied stimuli has any significant effect on T_a , which is explicitly explained in [11]. Fig. 5 shows the minimized quadratic errors E_{min} dependent on the normalized peak value $F_{\text{max}}/F_{\text{max},100\%}$, whereas $F_{\text{max},100\%}$ is the maximum value of the force response that has been generated at maximum stimulation intensity $u(t)$ at each subject.

Fig. 5 shows that a transfer function with identical real poles models the muscle twitch generated by RPMS better than the muscle twitch generated by fES. In both cases the fourth-order transfer function does not yield significant improvement compared to the third-order model. Therefore, the model order is chosen as $n = 3$. With Eq. (2) and with consideration of the time-delay T_1

$$G_a(s) = G'_a(s) e^{-sT_1} = \frac{T_{a,\text{opt}}}{2e^{-2}} \frac{1}{(1 + sT_{a,\text{opt}})^3} e^{-sT_1} \quad (4)$$

is obtained as description of the activation dynamics of a single muscle twitch.

In order to analyze the dispersion of the parameter T_a between the individual subjects, data of 12 additional subjects has been recorded. 2984 data sets of in total 20 subjects (aged from 20 to 35 years) have been evaluated. The average time constants $\bar{T}_{a,\text{opt},i}$ of each subject and its standard deviations $s_{T_{a,\text{opt},i}}$ have been calculated. The results are summarized in

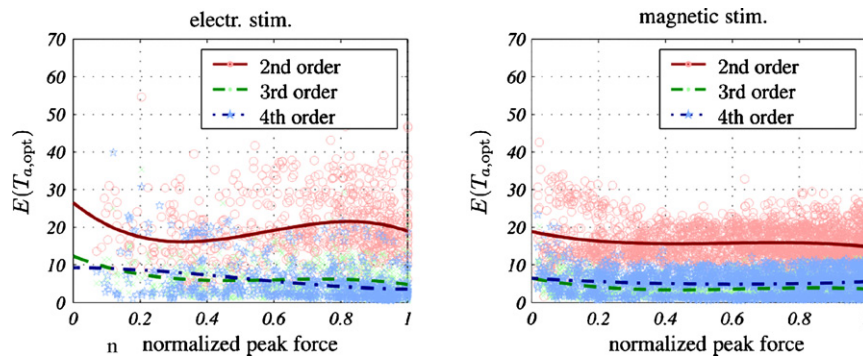


Fig. 5. Minimized quadratic errors E_{\min} dependent on the normalized peak value $F_{\max}/F_{\max,100\%}$.

Table 2. It can be seen that T_a varies a lot between the individual subjects, but the standard deviations within the particular subjects are small. The average time constants of all data sets are $\bar{T}_{a,opt} = 36.62$ ms for fES and $\bar{T}_{a,opt} = 38.44$ ms for RPMS.

Finally, the derived model is enhanced for repetitive stimulation. When applying repetitive stimuli the force responses begin to merge which results in a partial or complete tetanus (Fig. 6). This effect is called temporal summation. The pulse rate f_{rep} will be expressed as $k_{\text{rep}} = f_s/f_{\text{rep}}$. Based on Eq. (2) the discretized force response to a single magnetic stimulus can be written as

$$\hat{F}[k] = \begin{cases} 0 & \text{for } k < 0 \\ \frac{(kT_s)^2 e^{-kT_s/T_a}}{4T_a^2 e^{-2}} & \text{for } k \geq 0 \end{cases} \quad (5)$$

and for the temporal summation it follows

$$\hat{F}_{\text{rep}}[k] = \sum_{i=0}^{\infty} \hat{F}[k - ik_{\text{rep}}]. \quad (6)$$

From Fig. 6 it can be seen that in steady state, the superposition has a periodic part and a constant part \hat{F}_{rep} . The constant part \hat{F}_{rep} can be calculated as the average value of $\hat{F}_{\text{rep}}[k]$ over one repetition period at steady state. Assuming that

Table 2

Average time constants $\bar{T}_{a,opt,i}$ with standard deviation $s_{T_{a,opt,i}}$

	Electr. stim.	Magnetic stim.
$\bar{T}_{a,opt,i}$ (ms)	22.58–53.22	26.71–49.81
$s_{T_{a,opt,i}}$ (ms)	1.04–5.21	0.99–5.88

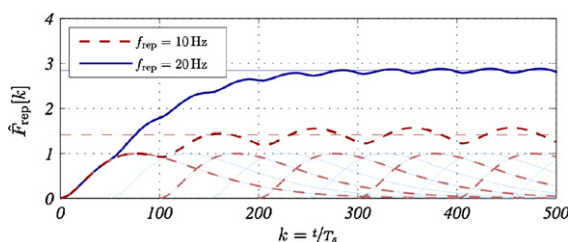


Fig. 6. Principle of temporal summation. During therapy, the repetition rate is typically chosen to $f_{\text{rep}} = 20$ Hz since this choice yields a good compromise between force generation and coil heating [11].

a muscle twitch is certainly decayed after 1 s or $k = f_s/1$ Hz, and hence, the steady state of the superposition (6) is reached (see also Fig. 6), \hat{F}_{rep} results in

$$\hat{F}_{\text{rep}} = \frac{1}{k_{\text{rep}}} \sum_{k=0}^{k_{\text{rep}}-1} \sum_{i=0}^{\infty} \hat{F}[k - ik_{\text{rep}} + \frac{f_s}{1\text{Hz}}] \approx \frac{1}{k_{\text{rep}}} \sum_{k=0}^{f_s/1\text{Hz}} \hat{F}[k]. \quad (7)$$

In Fig. 7 force responses of isometric muscle contractions with different repetition rates are depicted. It can be seen, that the constant values in steady state differ from those in Fig. 6 despite normalization with respect to the maximum peak value $F_{\max,100\%}$ measured at the muscle twitch of a single stimulus. This is due to the so-called nonlinear pulse rate dependent temporal summation. In Ref. [12] this is ascribed to the so-called “doublet effect”. To simplify the model structure this nonlinearity will be taken into account by modeling the nonlinear recruitment behavior in the subsequent section. For further analysis this nonlinearity will be compensated by normalizing the recorded muscle forces with respect to their respective constant values \bar{F}_{rep} . Fig. 8 shows that the average muscle contraction can be modeled very well with a reference function that has the average time constant $T_a = \bar{T}_{a,opt} = 38.44$ ms.

2.2. Recruitment behavior

The recruitment behavior describes the spatial summation of activated motor units and is mainly dependent on the stimulation intensity u . Since the nonlinear temporal summation has also to be taken into account, the recruitment behavior will be described with the two-dimensional function $\rho(u, f_{\text{rep}})$. In order to determine $\rho(u, f_{\text{rep}})$ the steady state force \bar{F}_{rep} has

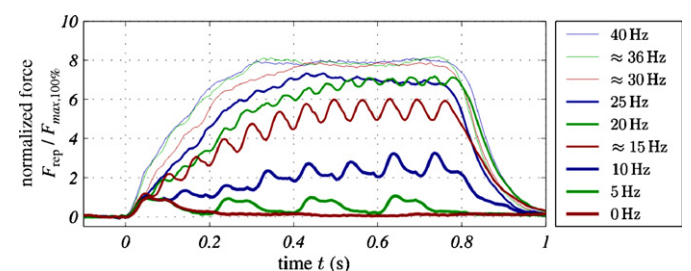


Fig. 7. Measured force response induced by RPMS at various pulse rates f_{rep} .

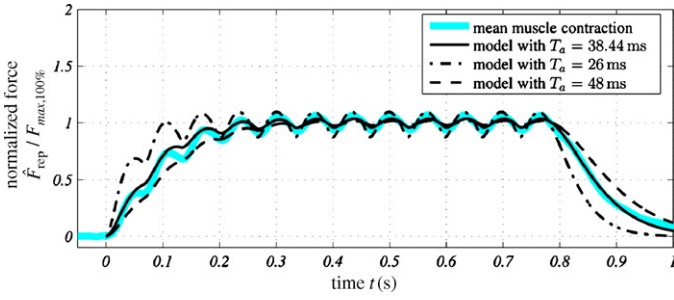


Fig. 8. Isometric muscle contraction induced by RPMS with $f_{\text{rep}} = 20$ Hz. The thick line is the mean measured contraction over all subjects.

been recorded under isometric conditions at intensities u from 0% to 100% and pulse rates f_{rep} from 15 Hz to 35 Hz. The results are depicted in Fig. 9. \bar{F}_{rep} has been normalized with respect to $\bar{F}_{\text{rep,max}}$ (measured at maximum stimulation intensity (100%) at a stimulation frequency of $f_{\text{rep}} = 20$ Hz) in order to obtain the relative recruitment. The experiment was conducted with seven healthy subjects and 882 data sets have been evaluated.

For the modeling approach it is assumed that the recruitment field of Fig. 9 can be analytically formulated as

$$\rho(u, f_{\text{rep}}) = \rho_u(u)\rho_f(f_{\text{rep}}) \quad (8)$$

where ρ_u describes the recruitment dependent on the stimulation intensity and ρ_f describes the component dependent on the repetition rate.

For the first factor of (8) the approximation (proposed in Ref. [13])

$$\rho_u(u) = \beta_1((u - u_{\text{thr}})\arctan(\alpha_{\text{thr}}(u - u_{\text{thr}})) - (u - u_{\text{sat}})\arctan(\alpha_{\text{sat}}(u - u_{\text{sat}})) + \beta_2) \quad (9)$$

is used.

Similar to ρ_u the dependency of the recruitment behavior on the stimulation frequency has been determined. The formula

$$\rho_f(f_{\text{rep}}) = \delta_1 \left(f_{\text{rep}} - (f_{\text{rep}} - f_{\text{sat}}) \cdot \left(\frac{1}{\pi} \arctan(\gamma_{\text{sat}}(f_{\text{rep}} - f_{\text{sat}})) + 0.5 \right) \right) + \delta_2 \quad (10)$$

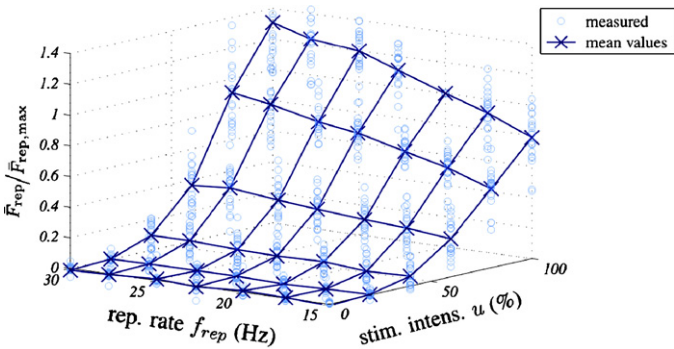


Fig. 9. Measured recruitment behavior.

Table 3

Parameters of Eqs. (9) and (10) to approximate the average relative recruitment of RPMS

	u_{thr}	$u_{\text{sat}}f_{\text{sat}}$	α_{thr}	$\alpha_{\text{sat}}\gamma_{\text{sat}}$	$\beta_1\delta_1$	$\beta_2\delta_2$
ρ_u	48%	98%	5	4	0.738	0.539
ρ_f	–	25 Hz	–	0.05	0.0597	–0.321

approximates the average nonlinear recruitment $\rho_{\text{rec},f}$. In order to approximate the measured recruitment field the parameters of Eqs. (9) and (10) have been adapted manually (Table 3). The comparison of the approximation (Fig. 10) with the measured recruitment field (Fig. 9) yields a good accordance.

2.3. Complete model

In order to obtain a complete model of the muscle contraction with RPMS the components of Sections 2.1 and 2.2 are integrated in a common model. Since the recruitment represents the number of recruited motor units, and the activation dynamics model the time response of the twitch of the respective motor units it seems appropriate to choose the order of the models as depicted in Fig. 11. This Hammerstein structure is also assumed for fES related models. Since the increase of the generated muscle force by increasing the repetition rate f_{rep} is already considered by the relative recruitment model $\rho_{u,\text{rep}}$, the overall model has to be normalized by the repetition rate dependent constant part $\hat{F}_{\text{rep}}(f_{\text{rep}})$. Taking this into consideration the overall model equation is

$$\hat{F}_{\text{rep},\rho}[k] = \hat{F}_{\text{rep}}[k - k_l] \frac{\rho(u, f_{\text{rep}})\bar{F}_{\text{rep,max}}}{\hat{F}_{\text{rep}}(f_{\text{rep}})} \quad (11)$$

whereas $\hat{F}_{\text{rep}}(f_{\text{rep}})$ is obtained by evaluating eq. (7) at $k_{\text{rep}} = f_s/f_{\text{rep}}$ and with the discretized latency $k_l = \text{ROUND}(T_l/T_s)$.

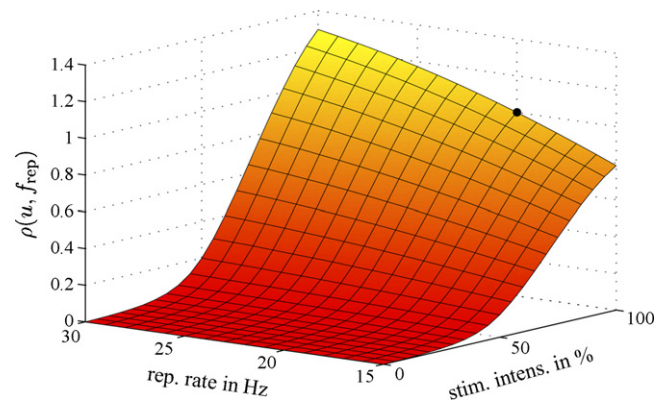


Fig. 10. Modeled recruitment.

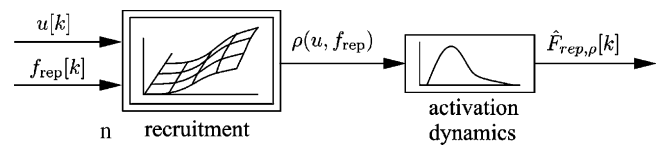


Fig. 11. Model of the induced muscle contraction in Hammerstein structure.

3. System identification

The parameters of the developed Hammerstein model do not only vary between subjects but depend on parameters like fitness, coil positions, etc. Therefore, a system identification method is proposed which adapts the model to a particular subject. The process of system identification can be divided into two steps: choice of the model structure and the model equation, respectively, and choice of parameter identification algorithm. In the following, basic definitions of this context will be briefly reviewed. Then, an identification method using a combination of a separable nonlinear regression approach with parameter reduction by means of orthonormal basis functions and a numerically robust modified recursive Levenberg–Marquardt algorithm is presented.

The parameter adaptation algorithms are derived in discrete time domain. Since all algorithms are implemented under quasi-continuous conditions (sample time $T_s = 1$ ms), the signal flow charts and transfer functions are expressed in continuous time and Laplace domain.

3.1. Model equation

3.1.1. Separable nonlinear regression model

A general discrete time equation of a nonlinear dynamic system with the output estimate $\hat{y}[k]$ can be written as

$$\hat{y}[k] = c(\underline{\varphi}[k], \underline{\theta}) \quad (12)$$

where c is a nonlinear function, $\underline{\varphi}[k]$ is the so-called input regressor, $\underline{\theta}$ a vector of the model parameters and with $k = t/T_s$. If $c(\underline{\varphi}[k], \underline{\theta})$ is of the form $c(\underline{\varphi}[k], \underline{\theta}) = \underline{\varphi}^T[k] \cdot \underline{\theta}$, i.e. the equation is linear in the parameters $\underline{\theta}$, a linear regression model is obtained. In this case, linear least squares methods can be applied for parameter identification. If the model Eq. (12) is nonlinear in its parameters $\underline{\theta}$, a nonlinear regression model is obtained and nonlinear local optimization methods have to be used for parameter identification. If the model (12) is linear function of some parameters and a nonlinear function of the rest it can be written as

$$\hat{y}[k] = \underline{\varphi}^T([k], \underline{\theta}_n) \cdot \underline{\theta}_1. \quad (13)$$

The parameter vector can be divided in linear parameters $\underline{\theta}_1$ and nonlinear parameters $\underline{\theta}_n$. This kind of model structure is called separable nonlinear regression model. For parameter identification one can make use of the separability feature which is explained in Section 3.2.1.

The most common structures of the input regressor $\underline{\varphi}[k]$ are $\underline{\varphi}[k] = [u[k] \ u[k-1] \ \dots \ u[k-n_u]]^T$, $\underline{\varphi}[k] = [y[k] \ y[k-1] \ \dots \ y[k-n_y]]^T$ and $\underline{\varphi}[k] = [y[k] \ y[k-1] \ \dots \ y[k-n_y] \ u[k] \ u[k-1] \ \dots \ u[k-n_u]]^T$ with the input and the output of the plant $u[k]$ and $y[k]$. According to the choice of the input regressor a (N)FIR, (N)AR or (N)ARX model is obtained. Good overviews and introductions on this topics can be found in Refs. [14,15].

3.1.2. Hammerstein cascade as separable nonlinear regression model

A Hammerstein cascade is a block structured system consisting of a static nonlinearity $n(u)$ in series with a linear dynamic element (Fig. 3). The LTI-system can be approximated as truncated convolution sum $\hat{y}[k] = \sum_{i=1}^m h[i]v(u[k-i])$ with the truncated impulse response $h[i]$. A main drawback of the convolution sum is the high number of m parameters which also depends on the sample time T_s . In order to reduce the number of parameters, $h[i]$ is expressed as a linear combination of orthonormal basis functions (OBFs) [15] with a reduced set of parameters $\underline{\theta}_i$:

$$h[i] = \sum_{l=1}^{m_r} \theta_{h,l} r_l[i]. \quad (14)$$

If the nonlinearity is approximated by a function that is linear in its parameters, such as a polynomial or a radial basis function network, a linear regression model for the entire Hammerstein cascade can be developed (e.g. [16]).

Approximating the nonlinearity $n(u)$ with a function $g(\underline{\theta}_g, u)$ that is nonlinear in its parameters $\underline{\theta}_g$ ($\underline{\theta}_g \in \mathbb{R}^{p \times 1}$), a separable nonlinear regression model can be obtained. The derivation in detail: using OBFs as parameter reduction method (Eq. (14)) and with $\underline{\theta} = [\underline{\theta}_h^T \ \underline{\theta}_g^T]^T$ the model output can be written as

$$\begin{aligned} \hat{y}(\underline{\theta}, u[k]) &= \sum_{i=1}^m \sum_{l=1}^{m_r} \theta_{h,l} r_l[i] \cdot v(u[k-i]) \\ &= \sum_{i=1}^m \sum_{l=1}^{m_r} \theta_{h,l} r_l[i] \cdot \underbrace{g(\underline{\theta}_g, u[k-i])}_{g[k-i]} \\ &= \sum_{l=1}^{m_r} \theta_{h,l} \sum_{i=1}^m r_l[i] g[k-i] \\ &= \sum_{l=1}^{m_r} \theta_{h,l} (r_l[0]g[k] + \dots + r_l[m]g[k-m]). \end{aligned} \quad (15)$$

With $\underline{g}[k] = [g[k] \ \dots \ g[k-m]]^T$ and with $\underline{u}[k] = [u[k] \ \dots \ u[k-m]]^T$ it follows

$$\begin{aligned} \hat{y}(\underline{\theta}, u[k]) &= \sum_{l=1}^{m_r} \theta_{h,l} (\underline{g}[k]^T \underline{r}_l) = \theta_{h,1} \underline{g}[k]^T \underline{r}_1 + \dots + \theta_{h,m_r} \underline{g}[k]^T \underline{r}_{m_r} \\ &= \underbrace{[\underline{g}[k]^T \ \underline{r}_1 \ \dots \ \underline{g}[k]^T \ \underline{r}_{m_r}]^T}_{\underline{\varphi}^T(\underline{\theta}_g, \underline{u}[k])} \underline{\theta}_h = \underline{\varphi}^T(\underline{\theta}_g, \underline{u}[k]) \underline{\theta}_h. \end{aligned} \quad (16)$$

Thus, a NFIR model is obtained that is parameterized with $p + m_r$ parameters.

3.2. Parameter identification algorithm

The optimal parameters $\underline{\theta}_{\min}$ are defined by the least squares problem

$$\underline{\theta}_{\min} = \arg \min_{\underline{\theta}} V(\underline{\theta}) \quad (17)$$

where the cost functional V is typically defined as

$$V_N(\underline{\theta}) = \frac{1}{2N} \sum_{k=1}^N e^2([k], \underline{\theta}) \quad (18)$$

with the output error $e([k], \underline{\theta}) = y[k] - \hat{y}([k], \underline{\theta})$. In the off-line case the quadratic sum (18) is calculated from a fixed data set of N input–output pairs $(y[k]|u[k])$. In the case of on-line identification where in each iteration a new data sample is available the criterion

$$V_k(\underline{\theta}) = \frac{1}{2} \sum_{\tau=1}^k \lambda^{k-\tau} e^2([k], \underline{\theta}) \quad (19)$$

is considered where $0 < \lambda < 1$ is the forgetting factor that determines the decay of past data samples. If a linear regression model is used, the optimization problem (17) can be solved by using linear least squares optimization which always leads to the global minimum. In the case of a nonlinear regression model local nonlinear optimization has to be applied. For separable nonlinear regression models Golub and Perreyra developed the so-called separable least squares algorithm [8] (SLS-algorithm) which will be briefly explained in the following section.

3.2.1. Separable least squares algorithm

With the vector/matrix notations

$$\underline{y} = \begin{bmatrix} y[1] \\ \vdots \\ y[N] \end{bmatrix} \text{ and } \Phi(\underline{\theta}_n) = \begin{bmatrix} \underline{\varphi}^T(\underline{\theta}_n, u[1]) \\ \vdots \\ \underline{\varphi}^T(\underline{\theta}_n, u[N]) \end{bmatrix} \quad (20)$$

the functional (18) of a separable nonlinear regression model (13) can be rewritten as

$$V_N(\underline{\theta}) = \frac{1}{2N} \|\underline{y} - \Phi(\underline{\theta}_n) \underline{\theta}_1\|_2^2 \quad (21)$$

With this notation it is easy to see that if we knew the nonlinear parameters $\underline{\theta}_n$ the linear parameters $\underline{\theta}_1$ could be calculated by solving the linear least squares problem

$$\underline{\theta}_1 = \Phi(\underline{\theta}_n)^+ \underline{y} \quad (22)$$

By replacing $\underline{\theta}_1$ in (21) with (22), a new cost function

$$\tilde{V}_N(\underline{\theta}_n) = \frac{1}{2N} \|\underline{y} - \Phi(\underline{\theta}_n) \Phi(\underline{\theta}_n)^+ \underline{y}\|_2^2 \quad (23)$$

is obtained, where the linear parameters have been eliminated. Golub and Perreyra set up the following theorem (proof see [8]):

If $\underline{\theta}_{n,\min}$ is a minimizer of $\tilde{V}_N(\underline{\theta}_n)$, and $\underline{\theta}_{l,\min} = \Phi^+(\underline{\theta}_{n,\min}) \underline{y}$, then, $\underline{\theta}_{\min} = [\underline{\theta}_{l,\min}^T \ \underline{\theta}_{n,\min}^T]^T$ also minimizes the original cost function $V_N(\underline{\theta})$ and thus, $\tilde{V}_N(\underline{\theta}_{n,\min}) = V_N(\underline{\theta}_{\min})$.

Therefore, the SLS-algorithm divides the calculation of $\underline{\theta}_{\min}$ in two steps:

1. Minimize $\tilde{V}_N(\underline{\theta}_n)$ in order to obtain $\underline{\theta}_{n,\min}$.

2. Use the optimal value $\underline{\theta}_{n,\min}$ to calculate $\underline{\theta}_{l,\min}$ with linear regression according to Eq. (22).

Hence, the minimization using an iterative nonlinear search algorithm can be accomplished within a reduced parameter set. In Ref. [17] it could be shown that it always converges faster than the minimization of the full functional.

3.2.2. On-line parameter identification with modified recursive Levenberg–Marquardt algorithm

One of the most successful iterative local optimization methods for nonlinear least squares problems is the Levenberg–Marquardt (LM) algorithm (see e.g. [18]). In Ref. [10] a recursive variant for on-line adaptation is introduced, and in Ref. [19] the methods of [10] are combined with the SLS-algorithm. In this section it will be shown how this algorithm has been modified in order to make it numerically robust, when dealing with redundantly or almost redundantly parameterized model equations. Such problems may arise if there are parameters that have locally only little influence on the model output in a region around the minimum.

First, the derivations in Refs. [10,19] are briefly summarized: consider the cost functional (19) and let $\underline{\theta}[k]$ be the latest available estimate that minimizes $V_{k-1}(\underline{\theta})$. The goal is, to compute $\underline{\theta}[k+1]$. Therefore, the second-order Taylor expansion L is considered as model of the behavior of V_k in the neighborhood of the current estimate $\underline{\theta}[k]$:

$$V_k(\underline{\theta}) \approx L_k(\underline{\theta}) = V_k(\underline{\theta}[k]) + V'_k(\underline{\theta}[k])[\underline{\theta} - \underline{\theta}[k]] + \frac{1}{2} [\underline{\theta} - \underline{\theta}[k]]^T V''_k(\underline{\theta}[k]) [\underline{\theta} - \underline{\theta}[k]]. \quad (24)$$

In order to find $\underline{\theta}[k+1]$, the minimum of the quadratic model function L is computed by setting $L' = 0$. Hence, the parameter update

$$\underline{\theta}[k+1] = \underline{\theta}[k] - [V''_k(\underline{\theta}[k])]^{-1} V'_k(\underline{\theta}[k])^T \quad (25)$$

is obtained. Since the load for computation of V'_k and V''_k will increase every time a new data sample is available, recursive formula for V'_k and V''_k are introduced, that can be reviewed in Ref. [10].

With these recursive formula the parameter update can be written as

$$\underline{\theta}[k+1] = \underline{\theta}[k] + H[k]^{-1} \underline{\psi}([k], \underline{\theta}[k]) e[k] \quad (26)$$

and

$$H[k] = \lambda H[k-1]^{-1} + \underline{\psi}([k], \underline{\theta}[k]) \underline{\psi}([k], \underline{\theta}[k])^T \quad (27)$$

whereas $H[k]$ is an approximation of the Hessian matrix $V''_k(\underline{\theta})$ and $\underline{\psi}([k], \underline{\theta}) = \partial/\partial \underline{\theta}(\hat{y}([k], \underline{\theta}))$. The derived algorithm corresponds to the off-line Gauss–Newton (GN) method and is called recursive GN method. By replacing $H[k]$ with the scaled identity matrix $1/\mu[k]I$ a recursive gradient search is obtained with the step length $\mu[k]$. By modifying $H[k]$ to $R[k] = H[k] + \delta[k]I$ a LM update is accomplished. The damping factor $\delta[k]$ decides whether to make an update step in GN direction (small $\delta[k]$) or a small step in gradient direction (big $\delta[k]$). In order to

adapt $\delta[k]$ the second-order approximation of (24) is evaluated with the gain ratio

$$\gamma = \frac{V_k(\underline{\theta}[k]) - V_k(\underline{\theta}[k+1])}{V_k(\underline{\theta}[k]) - L_k(\underline{\theta}[k+1])} = \frac{r_a}{r_p} \quad (28)$$

of the actual reduction r_a and the predicted reduction r_p of the cost function. For the on-line identification we propose the following update rules:

- If $0 < \gamma < \zeta$, the approximation L_k is bad, hence, increase δ according to $\delta[k+1] = \kappa \cdot \delta[k]$ in order to update $\underline{\theta}[k]$ more in gradient direction.
- If $\gamma < 1 - \zeta$, the approximation L_k is good, hence, decrease δ according to $\delta[k+1] = \delta[k]/\kappa$ in order to update $\underline{\theta}[k]$ more in gradient direction.
- If $\gamma < 0$, the update step would increase the cost function, hence, discard the parameter update and adjust $\delta[k+1] = \kappa \cdot \delta[k]$.

The design parameters ζ and κ are typically chosen as $0 < \zeta < 0.5$ and $1 < \kappa < 1.1$. In the off-line case a search algorithm is stopped, when the minimum is found. The on-line algorithm keeps running, since the location of the minimum might change. This may lead to nearly singular matrices $R[k]$ close the minimum, especially, when the cost function V_k has a plateau-like shape in a region around the minimum. If the model equation $\hat{y}(\underline{\theta}, u[k])$ is overparameterized $R[k]$ will always be singular at the minimum, since there exists an infinite number of solutions. But also with nearly redundant parameterization (little influence of some parameters on the model output) numerical problems might appear. In order to avoid singularities, it is proposed to evaluate a condition number of $R[k]$ before its inversion. The condition number $s_r[k]$ is calculated as the ratio $s_r[k] = \max(S_i[k])/\min(S_i[k])$ of the largest and the smallest of the singular values $S_i[k]$ of $R[k]$ (see e.g. [20]). Hence, before the parameters $\underline{\theta}[k]$ are updated, the following rule is applied

- If $s_r[k] > \xi$ the diagonal elements of $R[k]$ will be increased by adjusting $\delta[k]$ to $\delta[k] + \delta_s$.

The threshold ξ and δ_s have been chosen to $\xi = 1000$ and $\delta_s = 0.1$.

If the functional (23) is formulated according to the criterion (19) the recursive modified LM-algorithm can be applied to identify the nonlinear parameters $\underline{\theta}_n$ of an SLS-problem. The linear parameters are identified by solving Eq. (22) at every iteration by means of a recursive least squares algorithm. For an extensive derivation the reader is referred to [21,19].

3.3. Identification of RPMS-induced isometric muscle contraction

The parameter identification of the qualitative model introduced in Section 2 has been accomplished at the musculus extensor indicis proprius (index finger extensor) according to

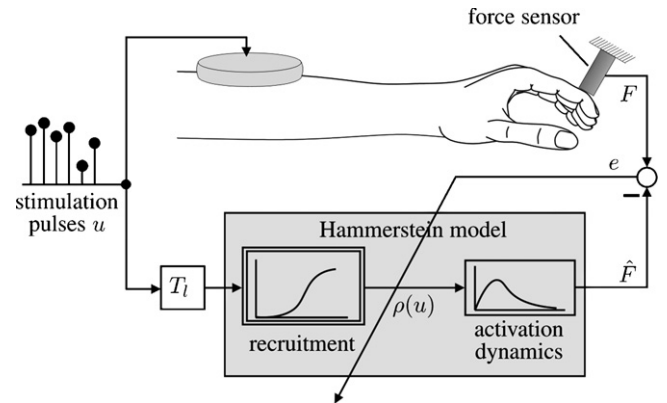


Fig. 12. Output error model for isometric parameter identification.

the output error configuration depicted in Fig. 12 using the modeling and identification methods described in Sections 3.1.2 and 3.2.2. In the following, firstly simulation results are shown in order to demonstrate the capability of the identification approach and secondly results with experimental data are given in order to show the applicability the real plant.

3.3.1. System excitation

The magnetic field pulses are applied at a constant repetition rate $f_{\text{rep}} = 20$ Hz. Hence, the identified recruitment behavior is a function of the stimulation intensity only. The duration of a magnetic pulse is $100 \mu\text{s}$ and hence, the input signal $u[k]$ can be approximated as discrete Dirac delta pulse train with a repetition rate k_{rep} :

$$u[k] = \sum_{i=0}^{\infty} a[k] \delta[k - ik_{\text{rep}}] \quad (29)$$

The amplitude of the Dirac delta pulses (i.e. the stimulation intensity) is modulated with the factor $a[k]$. For simulative identification, $a[k]$ is a uniformly distributed random variable with $0\% \leq a[k] \leq 100\%$. During the real experiments, a sinusoidal change (periodic time: 9 s) of the intensity between 0% and 100% is preferred, because the subjects had difficulties to relax the stimulated muscle during randomly changed intensities. Since the spectrum of a Dirac delta function is 1, the chosen input excites all frequencies of the plant. For nonlinear systems it is further required that all frequencies are excited in combination with all input amplitudes. Random as well as with sinusoidal change of intensity meet this requirement and hence, the system input can be considered as rich enough to cover all operating conditions of interest.

3.3.2. Model parameterization

The static nonlinearity $n(u)$ is approximated with the recruitment model (9) with gain $\beta_1 = 1$ and offset β_2 such that $\rho(\underline{\theta}_\rho, 0) = 0$. The gain parameter β_1 can be chosen constant, since the overall gain of the Hammerstein model can be adapted with the parameterization of the LTI system. The parameter vector is chosen to $\underline{\theta}_\rho = [u_{\text{sat}} \ u_{\text{thr}} \ \alpha_{\text{sat}}]^T$. Due to its small influence on the shape of ρ , the parameter α_{thr} has been chosen

constant to $\alpha_{\text{thr}} = 6$. Hence, we obtain

$$\begin{aligned} \rho(\underline{\theta}_\rho, u) &= (u - \underline{\theta}_{\rho,1}) \arctan(6(u - \underline{\theta}_{\rho,1})) \\ &\quad - (u - \underline{\theta}_{\rho,2}) \arctan(\underline{\theta}_{\rho,3}(u - \underline{\theta}_{\rho,2})) \\ &\quad + \underline{\theta}_{\rho,1} \arctan(-6\underline{\theta}_{\rho,1}) - \underline{\theta}_{\rho,2} \arctan(-\underline{\theta}_{\rho,3}\underline{\theta}_{\rho,2}). \end{aligned} \quad (30)$$

As OBFs, distorted sinusoidal functions are used, since weakly damped systems as well as strongly damped systems can be described with this type of functions [22,23]. The basis functions $\tilde{R} \in \mathbb{R}^{m_r \times m}$ are defined by

$$\tilde{r}_l[i] = \frac{1}{\sqrt{m/2}} \sin\left(l\pi \left(1 - \exp\left(\frac{-(i-0.5)}{\eta}\right)\right)\right) \quad (31)$$

$$\forall l = 1, \dots, m_r \text{ and } \forall i = 0, \dots, m$$

whereas m is the length of the truncated convolution sum, m_r the number of basis functions and $\eta \in \mathbb{R}$ is the so-called form factor that adapts the basis functions to the system dynamics. The function \tilde{R} are orthonormalized by a Cholesky decomposition according to $R = (C^T)^{-1} \tilde{R}$ with $C^T C = \tilde{R} \tilde{R}^T$ and $R \in \mathbb{R}^{m_r \times m}$.

3.3.3. Simulative results

In order to test the capabilities of the proposed algorithms, a simulated contraction model has been identified. The plant parameters have been chosen to $u_{\text{thr}} = 48\%$, $u_{\text{sat}} = 98\%$, $\alpha_{\text{sat}} = 4$ and $T_a = 38.44$ ms. The design parameters of the identification algorithm have been chosen according to Table 4. The initial parameter estimates $\theta_\rho[0]$ and $\theta_h[0]$ are set to $\theta_\rho[0] = [40\% \ 90\% \ 3]^T$ and $\theta_h[0] = \underline{0}$. Fig. 13 shows the parameter swarms during the recursive identification. In Fig. 14 the reconstruction is depicted. The algorithm converges after approx. 36 s and after this period the relative output error $\bar{e} = |F - \hat{F}|/|F|$ is below 0.1%.

3.3.4. Experimental results

For the experimental identification in total 8 data sets of two different subjects have been identified. Since little change of the position or orientation of the coils has a big effect on the recruitment behavior, every subject has been stimulated with two slightly different coil positions. Two data sets at each

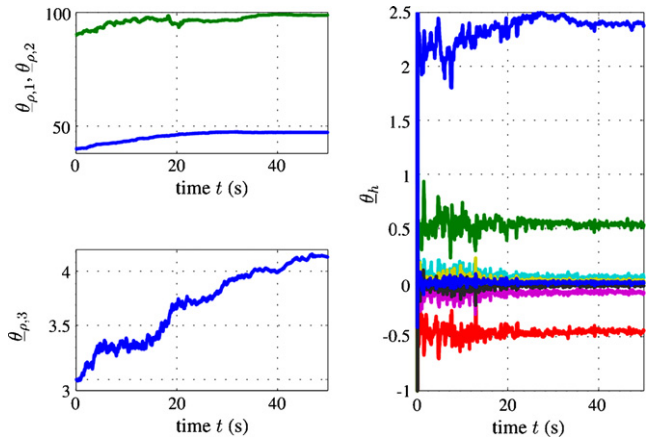


Fig. 13. Parameter swarms during simulated identification of the isometric force generation.

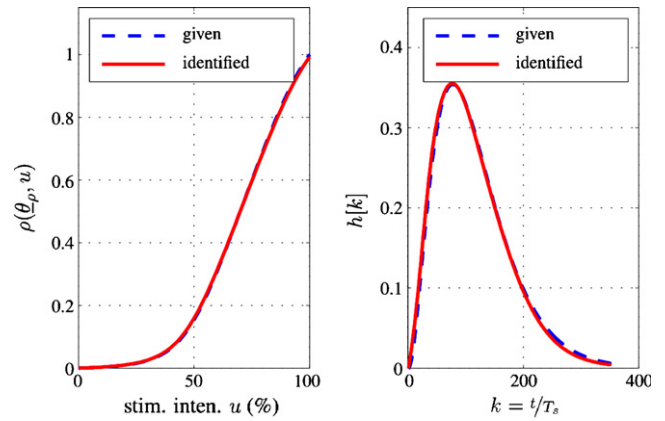


Fig. 14. Reconstructed identification results of the simulated output error configuration.

position have been recorded. This change of position should be reflected in the identification result of the recruitment behavior ρ . Since the stimulation sequences have not been longer than 90 s no notable muscle fatigue appears and hence, the plant can be considered as time invariant. The design parameters of the identification algorithm are summarized in Table 5. In order to make it easier to interpret the results of the reconstruction, the identified impulse responses $h[i]$ are normalized such that the stationary value \hat{F}_{rep} of the estimated force is 1, when activated

Table 4
Choice of design parameters for simulative identification

Modified LM-algorithm	
$\delta[0]$	0.001
$H[0]$	$0 < H_{i,j}[0] < 0.0001$, random uniform distribution
λ	0.99
κ	1.002
ζ	0.02
ξ	1000
δ_s	0.01
OBFs	
η	120
m	350
m_r	8

Table 5
Choice of design parameters for experimental identification

Modified LM-algorithm	
$\delta[0]$	0.001
$H[0]$	$0 < H_{i,j}[0] < 0.0001$, random uniform distribution
λ	0.999
κ	1.002
ζ	0.02
ξ	1000
δ_s	0.01
OBFs	
η	45
m	350
m_r	8

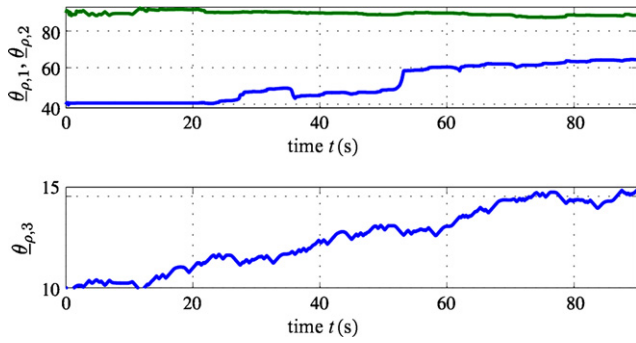


Fig. 15. Exemplary parameter swarm during identification of the isometric force generation with real data sets.

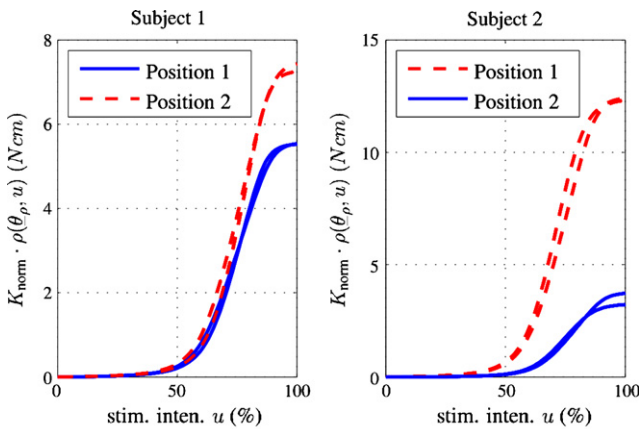


Fig. 16. Reconstructed recruitment characteristics $K_{\text{norm}} \cdot \rho$ of two subjects. Each subject has been stimulated twice at two slightly different coil positions.

with magnetic pulses of $f_{\text{rep}} = 20$ Hz and with a stimulation intensity of 100%. According to Eq. (7) this value can be calculated as $\hat{F}_{\text{rep}} = 20 \text{ Hz} \cdot T_s \sum_{i=0}^m h[i]$ so that the normalization factor K_{norm} can be calculated as $K_{\text{norm}} = 1/\hat{F}_{\text{rep}}$. In order to maintain the overall gain of the Hammerstein plant, the respective reconstructed recruitment ρ has to be multiplied by K_{norm} . Hence, the curve $K_{\text{norm}} \cdot \rho(u)$ directly indicates the stationary RPMS-induced muscle force depending on the stimulation intensity and with $f_{\text{rep}} = 20$ Hz.

The initial parameter estimates $\theta_\rho[0]$ and $\theta_h[0]$ are set to $\theta_\rho[0] = [40\% \ 90\% \ 10]^T$ and $\theta_h[0] = \underline{0}$. Fig. 15 shows an exemplary parameter swarm during the recursive identification. In Figs. 16 and 17 the reconstruction of the eight data sets is depicted. The obtained nonlinear parameters $\underline{\theta}_\rho$ are summarized in Table 6.

Table 6
Identified parameters $\underline{\theta}_\rho$ of eight data sets

	Subject 1				Subject 2			
	Coil pos. 1		Coil pos. 2		Coil pos. 1		Coil pos. 2	
$u_{\text{thr}}(\%)$	65.70	64.7	64.7	68.8	63.7	66.2	67.2	64.8
$u_{\text{sat}}(\%)$	85.5	86.9	87.5	87.5	81.7	87.4	83.9	93.1
α_{sat}	13.9	13.7	16.2	10.7	8.7	3.8	10.4	13.2

Two subjects have been stimulated four times, whereas the coils position has been slightly changed after two stimulation sessions.

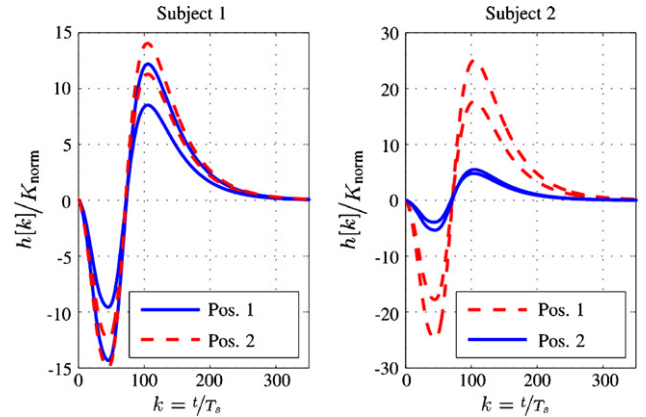


Fig. 17. Reconstructed impulse responses $h[k]/K_{\text{norm}}$ of two subjects.

The parameter adaptation converges after approx. 80 s and after this period the relative output error $\bar{e} = |F - \hat{F}|/|F|$ is below 1.5%.

3.4. Discussion

The proposed system identification allows a direct identification of the parameters of the qualitative model described in Section 2. Therefore, unlike approximating the nonlinearity with a polynomial or a artificial neural network, the identified parameters have an interpretable meaning and it is easier to chose good initial values, based on experience about what is physiologically suggestive. Furthermore the usage of a priori knowledge is maximized. Since the considered optimization problem is not convex and a local optimization method is used, the choice of initial parameters is essential for convergence to the global minimum. With simulations it could be shown that if the initial values are within a physiological reasonable area, the algorithm converges to the global minimum.

However, the incorporation of a priori knowledge results in small gradients of the error valley of the cost function $V_k(\underline{\theta})$ and to a locally redundant parameterization. These problems have been addressed with the proposed modified recursive Levenberg–Marquardt algorithm. When identifying with real data sets a relative output error of 1–1.5% is remaining. This is mainly due to model inconsistencies. The Hammerstein model is only a macroscopic approximation, that represents the dominant characteristics of the plant. The recruitment model $\rho(\underline{\theta}_\rho, u)$, e.g. has only three adaptive parameters and hence, a perfect approximation of the recruitment is not possible. However, looking at the identification results of the experiment with slightly different coil positions, obviously, the main characteristics of the recruitment behavior can be modeled and identified. The non-ideal recruitment model, non-ideal isometric conditions during the experiment, the simulated latency T_1 , uncomplete voluntary relaxation of the subjects during the experiment, etc. are model uncertainties that can not be reproduced by the idealized Hammerstein structure. Hence, the recursive least squares algorithm tries to compensate for these inconsistencies and yields an impulse response $h[i]$, that is

unphysiological. Therefore, it can be concluded, that the proposed approach allows to extract the important characteristics of the recruitment function at the cost of an insufficient identification of the impulse response.

4. Conclusion

A good model is only as detailed as necessary to sufficiently approximate the interesting characteristics of the original. The proposed algorithm identifies the main characteristics of the recruitment behavior and the system gain despite inconsistencies due to the idealized model. For our two main research goals position controlled movement induction and system identification based therapy monitoring, this is a sufficient model of the RPMS-induced muscle contraction. The developed on-line parameter identification can be applied during stimulation which is essential for an on-line monitoring of the patient parameters. In order to develop a spasticity quantification during stimulation, the proposed methods have to be enhanced for the non-isometric case, where the respective limb (e.g. the index finger) is moving. In this case the muscle force cannot be measured directly, and the joint angle of the limb is the system output (see e.g. [7]). Instead of estimating the force from position data, in Ref. [7] a neural observer [24] has been used in combination with a linear regression model for the RPMS-induced muscle contraction. In order to make use of the advantages of the SLS-identification, in the next step of ongoing research the presented methods will be combined with a neural observer.

Acknowledgement

This work has been supported by the Deutsche Forschungsgemeinschaft (DFG).

References

- [1] A. Struppler, P.M. Havel, P. Müller-Barna, Facilitation of skilled finger movements by repetitive peripheral magnetic stimulation (RPMS)—a new approach in central paresis, *NeuroRehabilitation* 18 (2003) 69–82.
- [2] A.B. Conforto, A. Kaelin-Lang, L.G. Cohen, Increase in hand muscle strength of stroke patients after somatosensory stimulation, *Ann. Neurol.* 51 (2002) 122–125.
- [3] A. Struppler, B.T. Angerer, C. Gündisch, P.M. Havel, Modulatory effect of repetitive peripheral magnetic stimulation (RPMS) on the skeletal muscle tone (stabilization of the elbow joint) on healthy subjects, *Exp. Brain Res.* 157 (1) (2004) 59–66.
- [4] P.H. Veltink, H.J. Chizeck, P.E. Crago, A. El-Bialy, Nonlinear joint angle control for artificially stimulated muscle, *IEEE Trans. Biomed. Eng.* 39 (1992) 368–380.
- [5] R. Riener, T. Fuhr, J. Quintern, G. Schmidt, A model for the design of fES standing-up strategies, in: *Proceedings of the 2nd Conference of the International Functional Electrical Stimulation Society (IFESS 1997)*, Burnaby, Canada (Valencia, CA, USA), IFESS, (August 1997), pp. 123–124.
- [6] T. Schauer, N. Negard, F. Prevedi, K. Hunt, M. Fraser, E. Ferchland, J. Raisch, Online identification and nonlinear control of the electrically stimulated quadriceps muscle, *Control Eng. Pract.* 13 (2005) 1207–1219.
- [7] M. Bernhardt, B.T. Angerer, M. Buss, A. Struppler, Neural observer based spasticity quantification during therapeutic muscle stimulation, in: *Proceedings of the 28th Annual International Conference of the IEEE Engineering in Medicine and Biology Society in New York*, August 30–September 3, IEEE EMBS, (September 2006), pp. 4897–4900.
- [8] H. Golub, V. Perreyra, The differentiation of pseudoinverses and nonlinear least squares problems whose variables are separate, *SIAM J. Numer. Anal.* 10 (1973) 413–432.
- [9] A. Ruhe, P. Wedin, Algorithms for separable nonlinear least squares problems, *SIAM Rev.* 22 (1980) 318–337.
- [10] L. Ljung, T. Söderström, *Theory and Practice of Recursive Identification*, vol. 4 of *The MIT Press Series in Signal Processing, Optimization, and Control*, MIT Press, Cambridge, MA, USA, 1987.
- [11] B.T. Angerer, *Fortschritte in der Erforschung der repetitiven peripheren Magnetstimulation*, Dissertation, Fakultät für Elektro- und Informationstechnik, Technische Universität München, München, Germany, January 2006.
- [12] R. Riener, J. Quintern, E. Psailer, G. Schmidt, Physiologically based multi-input model of muscle activation, in: A. Pedotti, M. Ferrarin, J. Quintern, R. Riener (Eds.), *Neuroprosthetics from Basic Research to Clinical Application*, Springer-Verlag, Heidelberg, Germany, 1996, pp. 95–114.
- [13] R. Riener, *Neurophysiologische und biomechanische Modellierung zur Entwicklung geregelter Neuroprothesen*, Dissertation, Fakultät für Elektro- und Informationstechnik, Technische Universität München, München, Germany, January 1997.
- [14] L. Ljung, *System Identification—Theory for the User*. PTR Prentice-Hall Information and System Sciences Series, 2nd ed., Prentice-Hall PTR, Upper Saddle River, NJ, USA, 1999.
- [15] O. Nelles, *Nonlinear System Identification—From Classical Approaches to Neural Networks and Fuzzy Models*, Springer-Verlag, Heidelberg, Germany, 2001.
- [16] B.T. Angerer, D. Schröder, A. Struppler, Nonlinear System Identification of Muscle Contractions Induced by Repetitive Peripheral Magnetic Stimulation, in *NOLCOS 2004—Stuttgart Symposium on Nonlinear Control Systems Preprints*, vol. 2, IFAC, VDI/VDE, (September 2004), pp. 669–674.
- [17] F.T. Krogh, Efficient implementation of a variable projection algorithm for nonlinear least squares problems, *Commun. ACM* 17 (3) (1974) 167–169.
- [18] J. Nocedal, S. Wright, *Numerical Optimization*, 2nd ed., Springer-Verlag, New York, USA, 1999.
- [19] L.S.H. Ngia, Separable nonlinear least-squares methods for efficient off-line and on-line modeling of systems using Kautz and Laguerre filters, *IEEE Trans. Circuits Syst.* 48 (2001) 562–579.
- [20] E. Anderson, Z. Bai, C. Bischof, S. Blackford, J. Demmel, J. Dongarra, J.D. Croz, A. Greenbaum, S. Hammarling, A. McKenney, D. Sorensen, *LAPACK User's Guide*, 3rd ed., SIAM, Philadelphia, USA, 1999.
- [21] L.S.H. Ngia, Separable nonlinear least-squares methods for on-line estimation of neural nets hammerstein models, *Neural Networks for Signal Processing X*, 2000. *Proceedings of the 2000 IEEE Signal Processing Society Workshop*, (December 2000), pp. 65–74.
- [22] A. Killich, *Prozeßidentifikation durch Gewichtsfolgeschätzung*, vol. 268 of *Fortschritt-Berichte VDI*, Reihe 8, VDI-Verlag, Düsseldorf, Germany, 1991.
- [23] B. Wahlberg, System identification using Laguerre models, *IEEE Trans. Autom. Control* 36 (1991) 551–562.
- [24] D. Schröder (Ed.), *Intelligent Observer and Control Design for Nonlinear Systems*, Springer-Verlag, Heidelberg, Germany, 2000.